LECTURE 14: Reflector Antennas

Introduction

High-gain antennas are required for long-distance radio communications (radio-relay links and satellite links), high-resolution radars, radioastronomy, etc. Reflector systems are probably the most widely used high-gain antennas. They can easily achieve gains of above 30 dB for microwave frequencies and higher. Reflector antennas operate on principles known long ago from the theory of geometrical optics (GO). The first reflector system was made by Hertz back in 1888 (a cylindrical reflector fed by a dipole). However, the art of accurately designing such antenna systems was developed mainly during the days of WW2 when numerous radar applications evolved.

18.3 m INTELSAT Earth Station (ANT Bosch Telecom), dual reflector

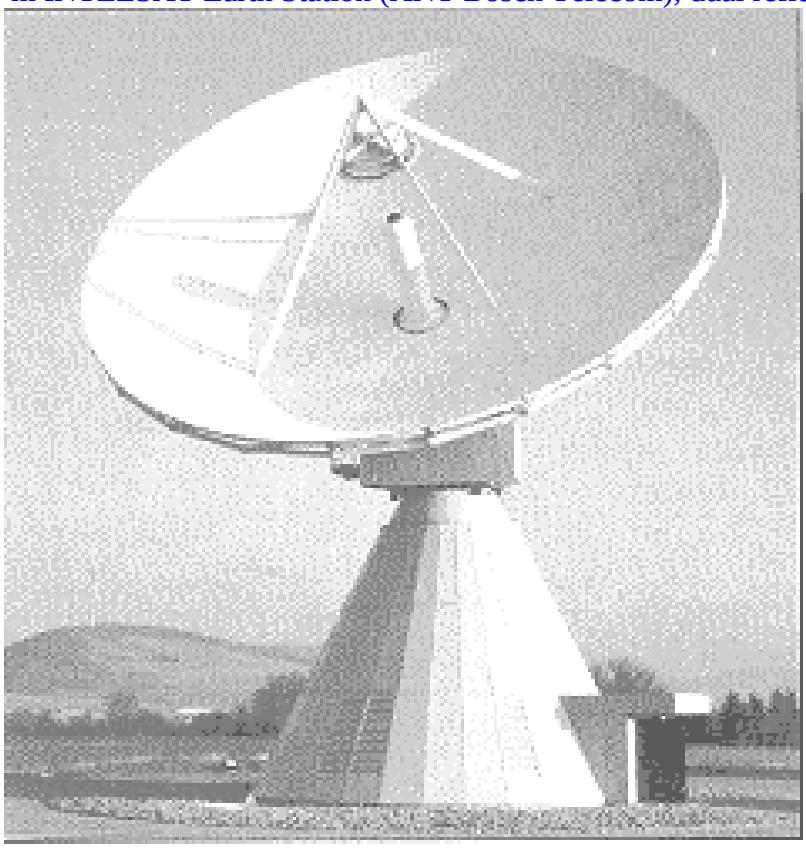

Aircraft radar

Radio relay tower

Feed-horn is in focal point

Conical horn primary feed

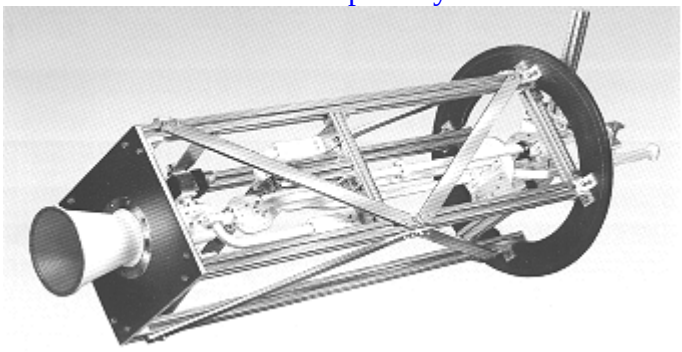

The simplest reflector antenna consists of two components: a reflecting surface and a much smaller feed antenna, which often is located at the reflector's focal point. Constructions that are more complex involve a secondary reflector (a subreflector) at the focal point, which is illuminated by a primary feed. These are called dual-reflector antennas. The most popular reflector is the parabolic one. Other reflectors often met in practice are: the cylindrical reflector, the corner reflector, spherical reflector, and others.

1. Principles of parabolic reflectors

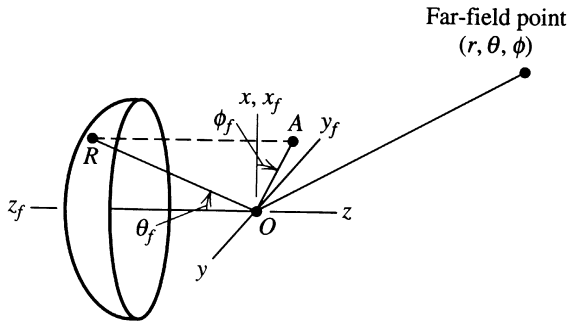

(*a*) Parabolic reflector and coordinate system

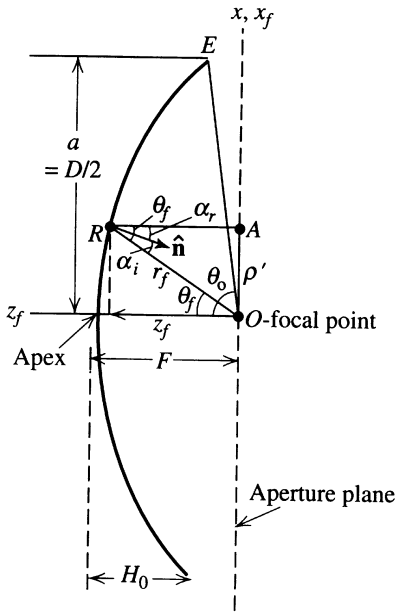

(*b*) Cross section of the reflector in the *xz*-plane.

A paraboloidal surface is described by the equation (see plot *b*):

$$\rho'^2 = 4F(F - z_f), \qquad \rho' \le a \tag{14.1}$$

Here, ρ' is the distance from a point *A* to the focal point *O*, where *A* is the projection of the point *R* on the reflector surface onto the axis-orthogonal plane (the aperture plane) at the focal point. For a given displacement ρ' from the axis of the reflector, the point *R* on the reflector surface is a distance r_f away from the focal point *O*. The position of *R* can be defined either by (ρ', z_f), which is a rectangular pair of coordinates, or by (r_f, θ_f), which is a polar pair of coordinates. A relation between (r_f, θ_f) and *F* is readily found from (14.1):

$$r_f = \frac{2F}{1+\cos\theta_f} = \frac{F}{\cos^2\left(\frac{\theta_f}{2}\right)} \tag{14.2}$$

Other relations to be used later are:

$$\rho' = r_f \sin\theta_f = \frac{2F\sin\theta_f}{1+\cos\theta_f} = 2F\tan\frac{\theta_f}{2} \qquad (14.3)$$

The axisymmetric paraboloidal reflector is rotationally symmetric and is entirely defined by the respective parabola, i.e. by two basic parameters: the diameter D and the focal length F. Often, the parabola is specified in terms of D and the ratio F/D. When F/D approaches infinity, the reflector becomes flat. Commonly used paraboloidal shapes are shown below. When $F/D = 0.25$, the focal point lies in the plane passing through the reflector's rim.

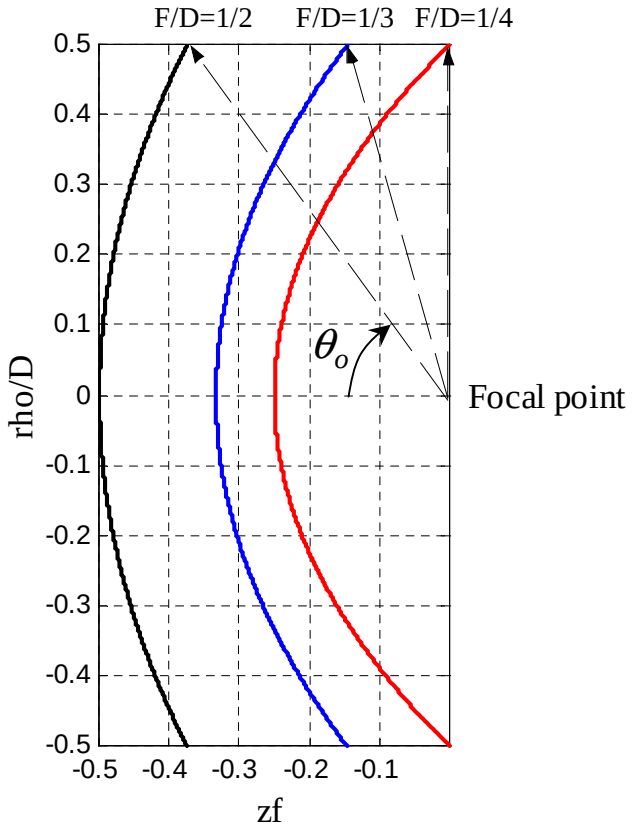

The angle from the feed (focal) point to the reflector's rim is related to F/D as:

$$\theta_o = 2\arctan\left[\frac{1}{4(F/D)}\right] \qquad (14.4)$$

The reflector design problem consists mainly of matching the feed antenna pattern to the reflector. The usual goal is to have the feed pattern at about a (–10) dB level in the direction of the rim, i.e. $F_f(\theta = \theta_o) = -10$ dB (0.316 of the normalized amplitude pattern). The focal distance *F* of a given reflector can be calculated after measuring its diameter *D* and its height H_0:

$$F = \frac{D^2}{16H_0} \tag{14.5}$$

(14.5) is found by solving (14.1) with $\rho' = D/2$ and $z_f = F - H_0$. For example, if $F/D = 1/4$, then $H_0 = D/4 \Rightarrow H_0 = F$, i.e. the focal point is on the reflector's rim plane.

The geometry of the paraboloidal reflector has two valuable features:

- All rays leaving the focal point *O* are collimated along the reflector's axis after reflection.
- All path lengths from the focal point to the reflector and on to the aperture plane are the same and equal to $2F$.

The above properties are proven by the GO methods, therefore, they are true only if the following conditions hold:

- The radius of the curvature of the reflector is large compared to the wavelength and the local region around each reflection point can be treated as planar.
- The radius of the curvature of the incoming wave from the feed is large and can be treated locally at the reflection point as a plane wave.
- The reflector is a perfect conductor, i.e. $\Gamma = -1$.

The collimating property of the parabolic reflector is easily established after finding the normal of the parabola.

$$\hat{n} = \frac{\nabla C_p}{\left|\nabla C_p\right|} \tag{14.6}$$

Here,

$$C_p = F - r_f \cos^2\left(\theta_f / 2\right) = 0 \tag{14.7}$$

is the parabolic curve equation (see equation (14.2)). After applying the ∇ operator in spherical coordinates):

$$\nabla C_p = -\hat{r}_f \cos^2\frac{\theta_f}{2} + \hat{\theta}_f \cos\frac{\theta_f}{2}\sin\frac{\theta_f}{2} \tag{14.8}$$

$$\Rightarrow \hat{n} = -\hat{r}_f \cos\frac{\theta_f}{2} + \hat{\theta}_f \sin\frac{\theta_f}{2} \tag{14.9}$$

The angles between $\hat{n}$ and the incident and reflected rays are found below.

$$\cos\alpha_i = -\hat{r}_f \cdot \hat{n} = \cos\frac{\theta_f}{2} \tag{14.10}$$

According to Snell's law, $\alpha_i = \alpha_r$. It is easy to show that this is fulfilled only if the ray is reflected in the *z*-direction:

$$\cos\alpha_r = \hat{z}\cdot\hat{n} = (-\hat{r}_f\cos\theta_f + \hat{\theta}_f\sin\theta_f)\cdot$$
$$\left(-\hat{r}_f\cos\frac{\theta_f}{2} + \hat{\theta}_f\sin\frac{\theta_f}{2}\right) = \tag{14.11}$$
$$= \cos\theta_f\cos\frac{\theta_f}{2} + \sin\theta_f\sin\frac{\theta_f}{2} \equiv \cos\frac{\theta_f}{2}$$

Thus, it was proven that for any angle of incidence θ_f the reflected wave is *z*-directed.

The equal path length property follows from (14.2). The total path-length *L* for a ray reflected at the point *R* is:

$$L = \overline{OR} + \overline{RA} = r_f + r_f\cos\theta_f = r_f(1+\cos\theta_f) = 2F \tag{14.12}$$

It is obvious that *L* is a constant equal to 2*F* regardless of the angle of incidence.

2. Aperture distribution analysis via GO (aperture integration)

There are two basic techniques to the analysis of the radiation characteristics of reflectors. One is called the *current distribution method*, which is a physical optics (PO) approximation. It assumes that the incident field from the feed is known, and that it excites surface currents on the reflector's surface as $\vec{J}_s = 2\hat{n}\times\vec{H}^i$. This

current density is then integrated to yield the far-zone field. It is obvious that PO method assumes perfect conducting surface and reflection from locally flat surface patch (it utilizes image theory). Besides, it assumes that the incident wave coming from the primary feed is locally plane far-zone field.

For the *aperture distribution method*, the field is first found over a plane, which is normal to the reflector's axis, and lies at its focal point (the *antenna aperture*). GO (ray tracing) is used to do that. Equivalent sources are formed over the aperture plane. It is assumed that the equivalent sources are zero outside the reflector's aperture. We shall first consider this method.

The field distribution at the aperture of the reflector antenna is necessary in order to calculate the far-field pattern, directivity, etc. Since all rays from the feed travel the same physical distance to the aperture, the aperture distribution will be of uniform phase. However, there is a non-uniform amplitude distribution. This is because the power density of the rays leaving the feed falls off as $1/r_f^2$. After the reflection, there is no spreading loss since the rays are collimated (parallel). Finally, the aperture amplitude distribution varies as $1/r_f$. This is explained in brief as follows.

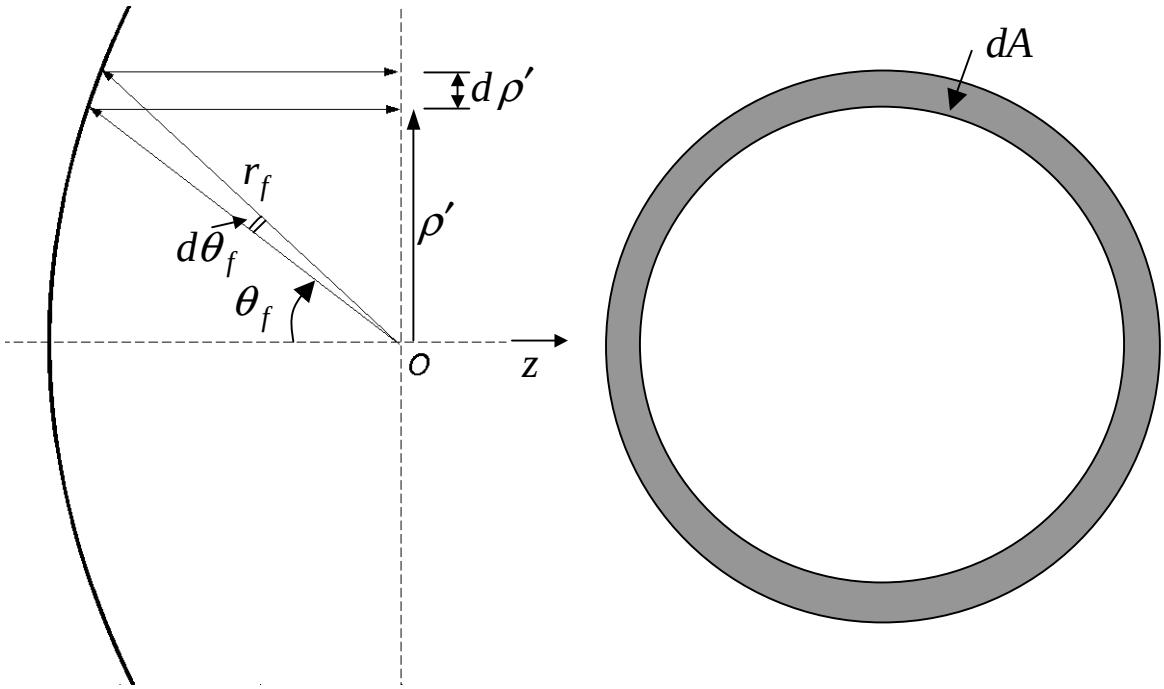

GO assumes that power density in free space follows straight-line paths. Applied to the power transmitted by the feed, the power in a conical wedge stays confined within as it progresses along the cone's axis. Let us consider a conical wedge of solid angle $d\Omega$ whose cross-section is of infinitesimal angle $d\theta_f$. It confines power, which after being reflected from the paraboloid, arrives at the aperture plane confined within a cylindrical ring of thickness $d\rho'$ and area $dA = 2\pi\rho' d\rho'$.

Let us assume that the feed is isotropic and it has radiation intensity $U = \Pi_t / 4\pi$, where Π_t is the transmitted power. The power confined in the conical wedge is $d\Pi = Ud\Omega = \frac{\Pi_t}{4\pi} d\Omega$. This power reaches the aperture plane with a density of

$$P_a(\rho') = \frac{d\Pi}{dA} = \frac{\Pi_t}{4\pi}\frac{d\Omega}{dA} \tag{14.13}$$

The generic relation between the solid angle increment and the directional angles' increments is

$$d\Omega = \sin\theta d\theta d\varphi \tag{14.14}$$

(see Lecture 4). In this case, the structure is rotationally symmetrical, so we define the solid angle of the conical wedge as:

$$d\Omega = \int_0^{2\pi} (\sin\theta_f d\theta_f) d\varphi_f = 2\pi \sin\theta_f d\theta_f \tag{14.15}$$

Substituting (14.15) and $dA = 2\pi\rho' d\rho'$ in (14.13) gives:

$$P_a(\rho') = \frac{\Pi_t}{4\pi}\frac{2\pi\sin\theta_f d\theta_f}{2\pi\rho' d\rho'} = \frac{\Pi_t}{4\pi}\frac{\sin\theta_f}{\rho'}\frac{d\theta_f}{d\rho'} \tag{14.16}$$

From (14.3), it is seen that

$$\frac{d\rho'}{d\theta_f} = \frac{F}{\cos^2(\theta_f/2)} = r_f \tag{14.17}$$

$$\Rightarrow \frac{d\theta_f}{d\rho'} = \frac{1}{r_f} \tag{14.18}$$

$$\Rightarrow P_a(\rho') = \frac{\Pi_t}{4\pi} \frac{\sin\theta_f}{\underbrace{r_f \sin\theta_f}_{\rho'}} \frac{1}{r_f} = \frac{\Pi_t}{4\pi} \frac{1}{r_f^2} \tag{14.19}$$

Equation (14.19) shows the spherical nature of the feed radiation, and it is referred to as *spherical spreading loss*. Since $E_a \propto \sqrt{P_a}$,

$$E_a \propto \frac{1}{r_f} \tag{14.20}$$

Thus, there is a natural amplitude taper due to the curvature of the reflector. If the primary feed is not isotropic, the effect of its normalized field pattern $F_f(\theta_f, \varphi_f)$ is easily incorporated in (14.20) as

$$E_a \propto \frac{F_f(\theta_f, \varphi_f)}{r_f} \tag{14.21}$$

Thus, one can conclude that the field phasor at the aperture is:

$$E_a(\theta_f, \varphi_f) = E_m e^{-j\beta 2F} \cdot \frac{F_f(\theta_f, \varphi_f)}{r_f} \tag{14.22}$$

The coordinates (ρ', φ') are more appropriate for the description of the aperture field distribution. Obviously, $\varphi' \equiv \varphi_f$. As for r_f and θ_f, they are transformed as:

$$r_f = \frac{4F^2 + \rho'^2}{4F} \tag{14.23}$$

$$\theta_f = 2\arctan\frac{\rho'}{2F} \tag{14.24}$$

The last thing to be determined is the polarization of the aperture field provided the polarization of the primary-feed field is known (denoted with $\hat{u}_i$). The law of reflection at a perfectly conducting wall states that $\hat{n}$ bisects the incident and the reflected rays, and that the total electric field has zero tangential component at the surface:

$$\vec{E}_\tau^{\,i} + \vec{E}_\tau^{\,r} = 0 \tag{14.25}$$

and

$$\vec{E}^r + \vec{E}^i = 2(\hat{n}\cdot\vec{E}^i)$$
$$\Rightarrow \vec{E}^r = 2(\hat{n}\cdot\vec{E}^i) - \vec{E}^i \qquad (14.26)$$

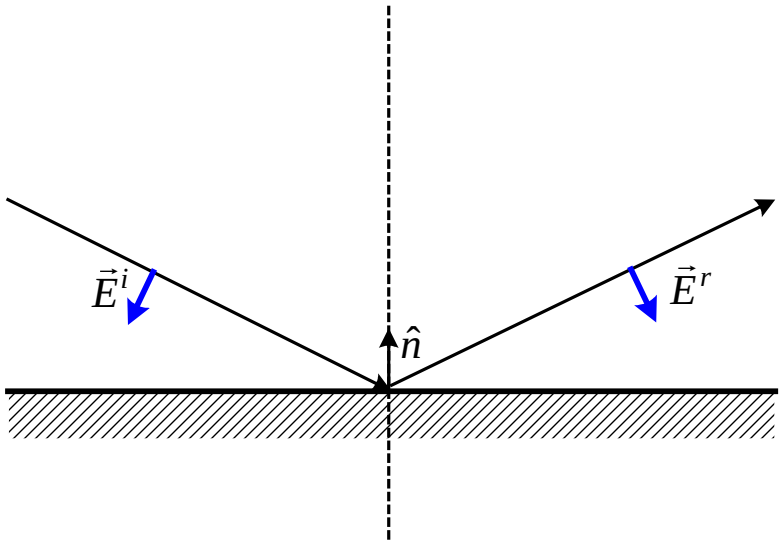

Since we have full reflection (perfect conductor), $|\vec{E}^i| = |\vec{E}^r|$. Then,

$$\hat{u}_r = 2(\hat{n}\cdot\hat{u}_i)\hat{n} - \hat{u}_i \qquad (14.27)$$

Here, $\hat{u}_i$ is the unit vector of the incident ray, and $\hat{u}_r$ is the unit vector of the reflected ray. The aperture field distribution is fully defined by (14.22) and (14.27). The radiation integral over the electric field can be now formed. For example, a circular paraboloid would have a circular aperture, and the radiation integral becomes:

$$\vec{\mathcal{J}}^E = E_m \int_0^{2\pi}\int_0^{D/2} \frac{F_f(\rho',\varphi')}{r_f}\hat{u}_r e^{j\beta\rho'\sin\theta\cos(\varphi-\varphi')}\rho' d\rho' d\varphi' \qquad (14.28)$$

In the above considerations, it was said that the aperture field has uniform phase distribution. This is true only if the feed is located at the focal point. However, more sophisticated designs often use an offset feed. In such cases, the PO method (i.e. the current distribution method) is preferred.

3. The current distribution (PO) method (surface integration)

The basic description of this approach and its assumptions were already given in the previous section. Once the induced surface currents $\vec{J}_s$ are found, the magnetic vector potential $\vec{A}$ and the far-zone field can be calculated. In practice, the electric far field is calculated directly from $\vec{J}_s$ by

$$\vec{E}^{far} = -j\omega\mu \frac{e^{-j\beta r}}{4\pi r} \iint_{S_r} \underbrace{\left[\vec{J}_s - \left(\vec{J}_s \cdot \hat{r}\right)\hat{r}\right]}_{\vec{J}_{s/\perp\hat{r}}} e^{j\beta \hat{r}\cdot\vec{r}'} ds' \qquad (14.29)$$

Equation (14.29) follows directly from the relation between the far-zone electric field and the magnetic vector potential $\vec{A}$:

$$\vec{E}^{far} = -j\omega \vec{A}_{/\perp_{\hat{r}}}, \qquad (14.30)$$

which can written more formally as:

$$\vec{E}^{far} = -j\omega\vec{A} - (-j\omega\vec{A}\cdot\hat{r})\hat{r} = -j\omega(A_\theta\hat{\theta} + A_\varphi\hat{\varphi}) \qquad (14.31)$$

This approach is also known as Rusch's method after the name of the person who first introduced it. The integral in (14.29) has analytical solution for symmetrical reflectors, but it is usually evaluated numerically in practical computer codes, in order to render the approach versatile wrt any apertures.

In conclusion to this general discussions, it should be noted that both methods produce very accurate results for the main beam and first side lobe. The pattern far out the main beam can be accurately predicted by including diffraction effects (scattering) from the reflector's rim. This is done by augmenting GO with the use of *geometrical theory of diffraction* (GTD) (J.B. Keller, 1962), or by augmenting the PO method with the *physical theory of diffraction* (PTD) (P.I. Ufimtsev, 1957).

4. The focus-fed axisymmetric parabolic reflector antenna

This is a popular reflector antenna, whose analysis will be used to illustrate the general approach to the analysis of any reflector antenna. Consider a linearly polarized feed, with the $\vec{E}$ field along the *x*-axis. As before, the reflector's axis is along *z*. Let us also assume that the pattern of the feed is represented by

$$\vec{E}_f(\theta_f,\varphi_f) = E_m \frac{e^{-j\beta r_f}}{r_f}\left[\hat{\theta}_f\, C_E(\theta_f)\cos\varphi_f - \hat{\varphi}_f\, C_H(\theta_f)\sin\varphi_f\right] \quad (14.32)$$

Here, $C_E(\theta_f)$ and $C_H(\theta_f)$ denote its principal-plane patterns. The expression in (14.32) is a common way to approximate a 3-D pattern of an *x*-polarized antenna by knowing only the two principal-plane 2-D patterns. This approximation is actually very accurate for aperture-type antennas because it directly follows from the expression of the far-zone fields in terms of the radiation integrals (see Lecture 10, Section 3):

$$E_\theta = j\beta\frac{e^{-j\beta r}}{4\pi r}[\boxed{\mathcal{I}_x^E\cos\varphi} + \mathcal{I}_y^E\sin\varphi + \eta\cos\theta\left(\mathcal{I}_y^H\cos\varphi - \mathcal{I}_x^H\sin\varphi\right)] \quad (14.33)$$

$$E_\varphi = j\beta\frac{e^{-j\beta r}}{4\pi r}[-\eta(\mathcal{I}_x^H\cos\varphi + \mathcal{I}_y^H\sin\varphi) + \cos\theta\left(\mathcal{I}_y^E\cos\varphi\boxed{-\mathcal{I}_x^E\sin\varphi}\right)] \quad (14.34)$$

The aperture field will be now derived in terms of *x*- and *y*-components. To do this, the GO method of Section 2 will be used. An incident field of $\hat{u}_i = \hat{\theta}_f$ polarization will produce an aperture reflected field of the following polarization (see (14.27)):

$$\hat{u}_r^\theta = 2(\hat{n}\cdot\hat{\theta}_f)\hat{n} - \hat{\theta}_f = 2\sin\frac{\theta_f}{2}\hat{n} - \hat{\theta}_f =$$

$$= 2\sin\frac{\theta_f}{2}\left(\hat{r}_f\cos\frac{\theta_f}{2} + \hat{\theta}_f\sin\frac{\theta_f}{2}\right) - \hat{\theta}_f$$

$$\Rightarrow \hat{u}_r^{\theta} = -\hat{r}_f\left(2\sin\frac{\theta_f}{2}\cos\frac{\theta_f}{2}\right)-\hat{\theta}_f\left(1-2\sin^2\frac{\theta_f}{2}\right)= \tag{14.35}$$

$$= -\hat{r}_f\sin\theta_f - \hat{\theta}_f\cos\theta_f$$

Similarly, an incident field of $\hat{u}_i = \hat{\varphi}_f$ polarization will produce an aperture reflected field of the following polarization

$$\hat{u}_r^{\varphi} = -\hat{\varphi}_f \tag{14.36}$$

Transforming (14.35) and (14.36) to rectangular (x and y) coordinates at the aperture plane gives:

$$\begin{aligned}\hat{u}_r^{\theta} &= -\hat{x}\cos\varphi_f - \hat{y}\sin\varphi_f \\ \hat{u}_r^{\varphi} &= +\hat{x}\sin\varphi_f - \hat{y}\cos\varphi_f\end{aligned} \tag{14.37}$$

Superimposing the contributions of the $\hat{\theta}_f$ and $\hat{\varphi}_f$ components of the field in (14.32) to the aperture field x and y components produces:

$$\begin{aligned}&\vec{E}_a(\theta_f,\varphi_f) = E_m\frac{e^{-j\beta 2F}}{r_f}\times \\ &\{-\hat{x}\left[C_E(\theta_f)\cos^2\varphi_f + C_H(\theta_f)\sin^2\varphi_f\right] \\ &\quad -\hat{y}\left[C_E(\theta_f)-C_H(\theta_f)\right]\sin\varphi_f\cos\varphi_f\}\end{aligned} \tag{14.38}$$

In (14.38), the magnitude and phase of the vector are expressed as in (14.22). Note that a y-component appeared in the aperture field, despite the fact that the feed generates only E_x field. This is called *cross-polarization*. If the feed has rotationally symmetric pattern, i.e. $C_E(\theta_f) = C_H(\theta_f)$, there is no cross-polarization. From equation (14.38), it is also obvious that cross-polarization is zero at $\varphi_f = 0^\circ$ (E-plane) and at $\varphi_f = 90^\circ$ (H-plane). Cross-polarization is maximum at $\varphi_f = 45^\circ, 135^\circ$. Cross-polarization in the aperture means cross-polarization of the far field, too. Cross-polarization is unwanted because it could lead to polarization losses depending on the transmitting and receiving antennas.

It is instructive to examine (14.38) for a specific simple example: reflector antenna fed by a very short *x*-polarized electric dipole. Its principal-plane patterns are $C_E(\theta_f)=\cos\theta_f$ and $C_H(\theta_f)=1$. Therefore, it will generate the following aperture field:

$$\vec{E}_a = E_m \frac{e^{-j\beta 2F}}{r_f}\times\{-\hat{x}\left[\cos\theta_f\cos^2\varphi_f+\sin^2\varphi_f\right] - \hat{y}\left[\cos\theta_f-1\right]\sin\varphi_f\cos\varphi_f\} \qquad (14.39)$$

An approximate plot of the aperture field of (14.39) is shown below.

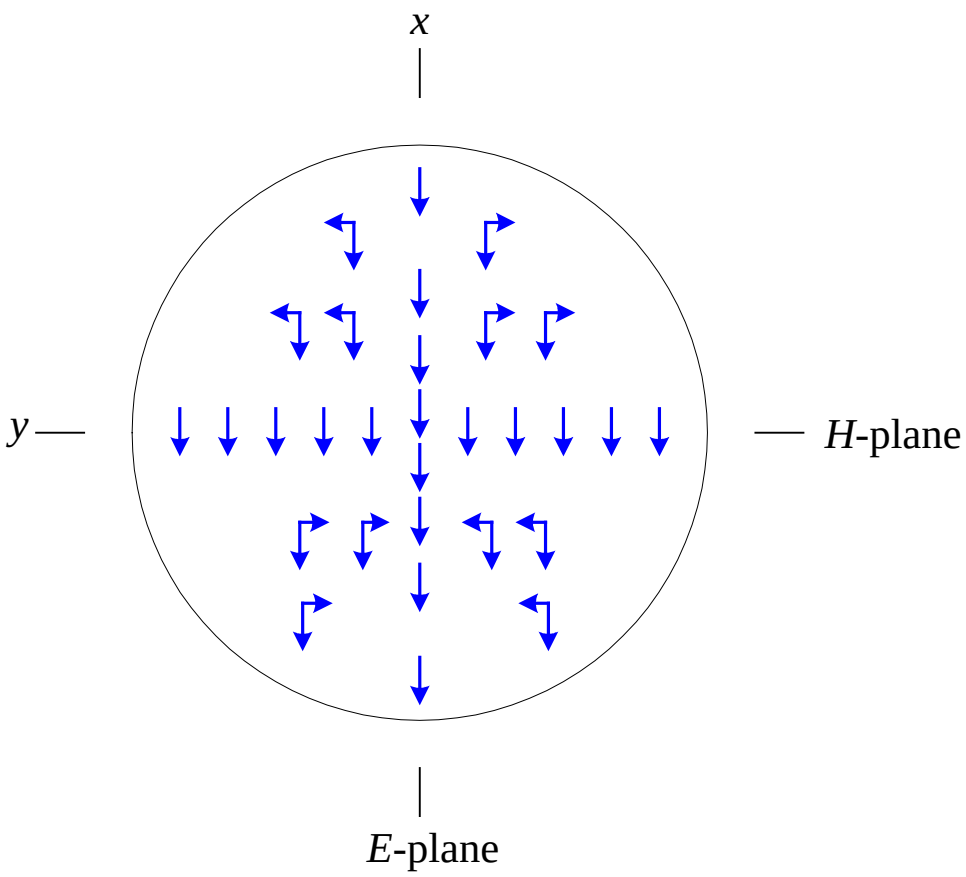

It must be also noted that cross-polarization decreases as the ratio F/D increases. This follows from (14.4), which gives the largest feed angle $\theta_{f_{\max}}=\theta_o$. As F/D increases, θ_o decreases, which

makes the cross-polarization term in (14.39) smaller. Unfortunately, large F/D ratios are not very practical.

An example is presented in W.L. Stutzman, G. Thiele, *Antenna Theory and Design*, of an axisymmetric parabolic reflector with diameter $D = 100\lambda$ and $F/D = 0.5$, fed by a half-wavelength dipole located at the focus.

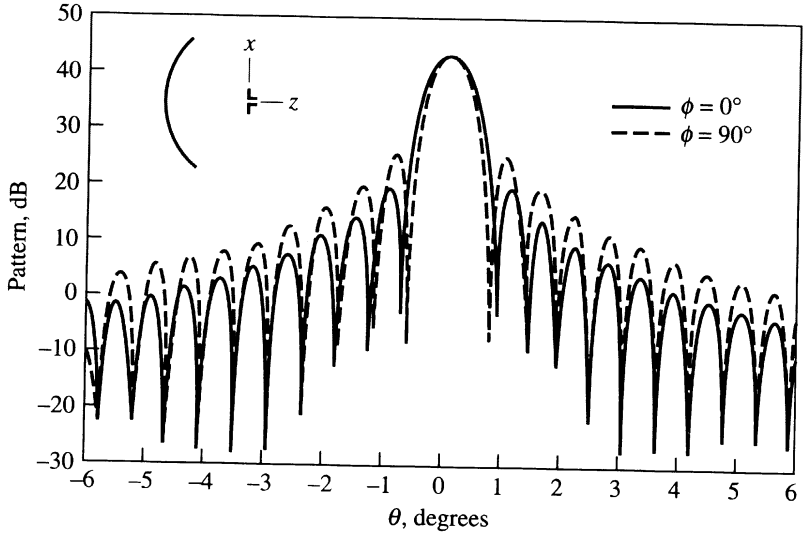

(*a*) Principal plane patterns.

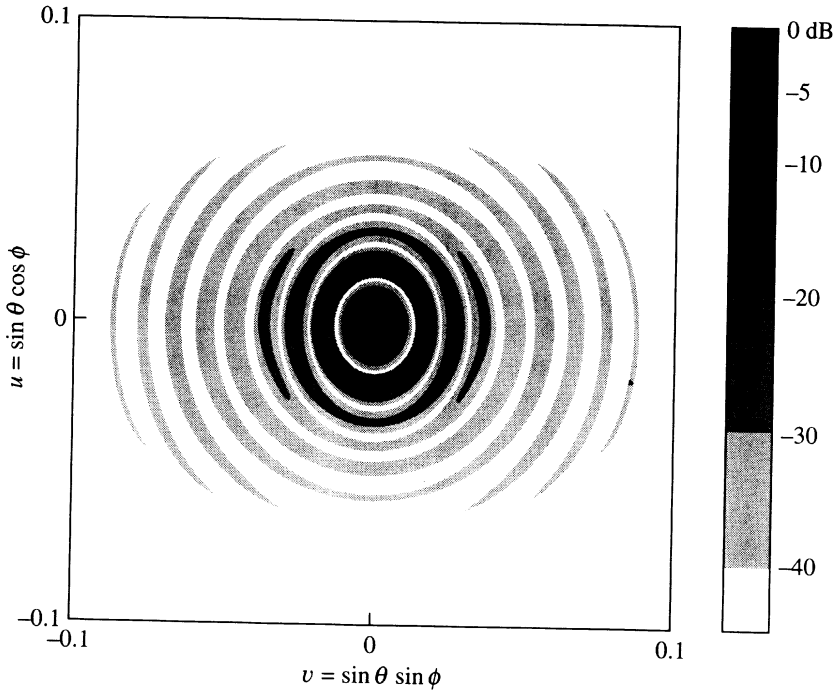

(*b*) Co-polar contours (normalized)

Cross-polarization:

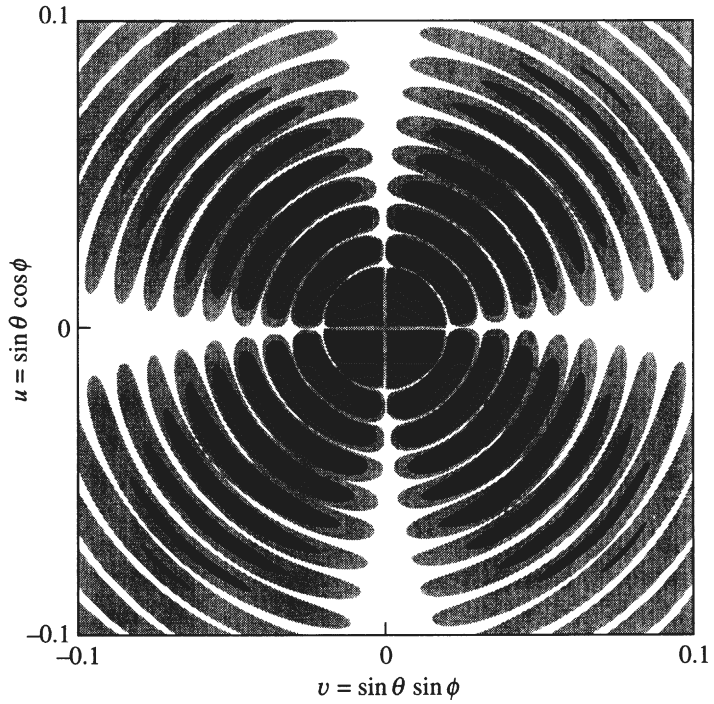

(*c*) Cross-polarization contours (normalized)

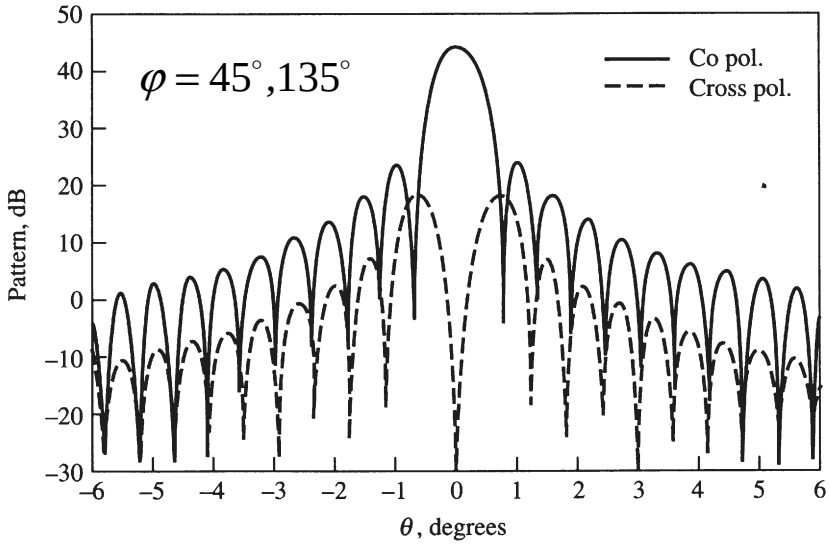

The results above are obtained using commercial software (GRASP) using PO methods (surface current integration).

Cross-polarization of reflectors is measured as the ratio of the peak cross-polarization far-field component to the peak co-polarization far field. For example, the above graph shows a cross-polarization level of *XPOL*=-26.3 dB.

5. Offset parabolic reflectors

One unpleasant feature of the focus-fed reflector antennas is that part of the aperture is blocked by the feed itself. To avoid this, offset-feed reflectors are developed, where the feed antenna is away from the reflector's aperture. They are developed as a portion of the so-called *parent reflector*. The price to pay is the increase of *XPOL*. That is why such reflectors are usually fed with primary feeds of rotationally symmetrical patterns, i.e. $C_E \approx C_H$, which effectively eliminates cross-polarization.

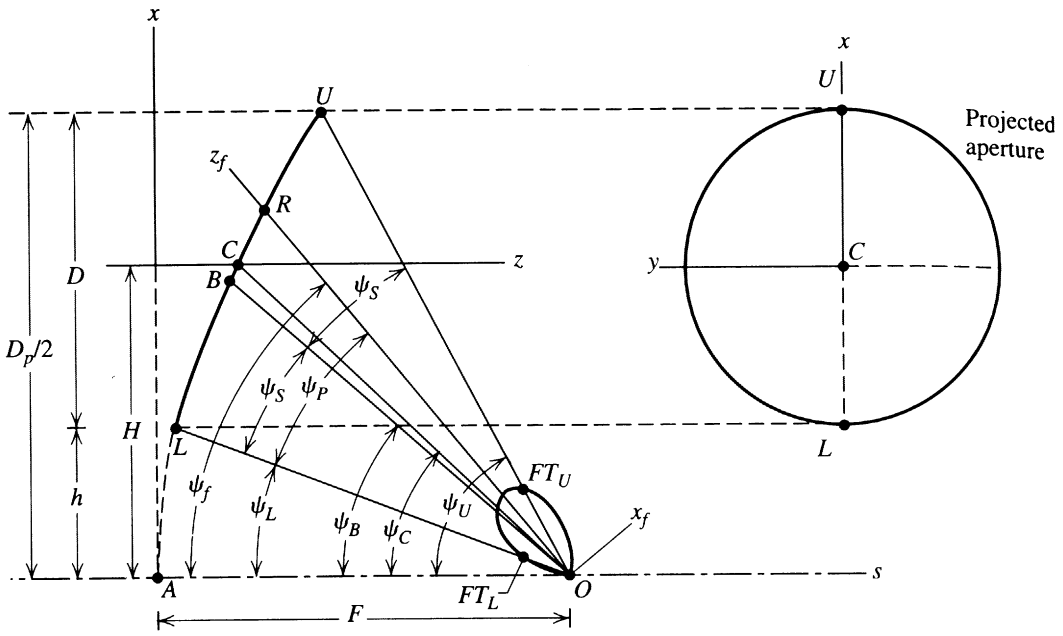

The analysis techniques given in the previous sections are general and can be applied to these reflectors, too. Generally, the PO method (surface currents integration) is believed to yield better accuracy. Both, the PO and the GO methods, are accurate only at the main beam and the first couple of side-lobes.

Offset reflectors are popular for antenna systems producing *contour beams*. Then, multiple primary feeds (usually horns) are illuminating the reflector at different angles, and constitute a significant obstacle at the antenna aperture.

6. Dual-reflector antennas

The dual-reflector antenna consists of two reflectors and a feed antenna. The feed is conveniently located at the apex of the main reflector. This makes the system mechanically robust, the transmission lines are shorter and easier to construct (especially in the case of waveguides).

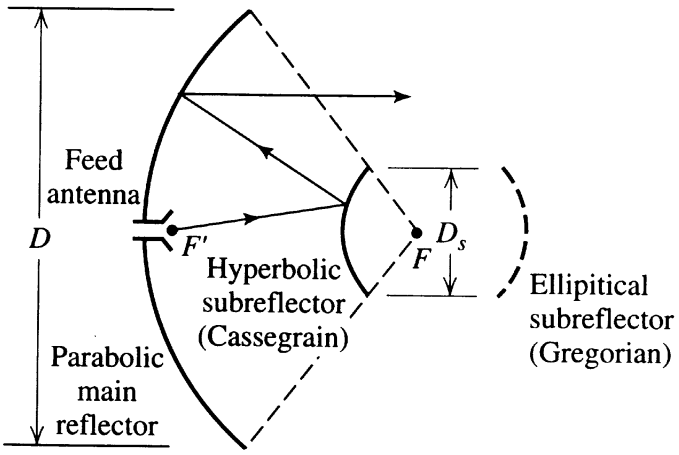

The virtual focal point *F* is the point from which transmitted rays appear to emanate with a spherical wave front after reflection from the subreflector.

The most popular dual reflector is the axisymmetric *Cassegrain* antenna. The main reflector is parabolic and the subreflector is hyperbolic (convex). A second form of the dual reflector is the *Gregorian* reflector. It has a concave elliptic subreflector. The Gregorian subreflector is more distant from the main reflector and, thus, it requires more support. Dual-reflector antennas for earth terminals have another important advantage, beside the location of the main feed. They have almost no spillover toward the noisy ground, as do the single-feed reflector antennas. Their spillover (if any) is directed toward the much less noisy sky region. Both, the

Cassegrain and the Gregorian reflector systems, have their origins in optical telescopes and are named after their inventors.

The subreflectors are rotationally symmetric surfaces obtained from the curves shown below (a hyperbola and an ellipse).

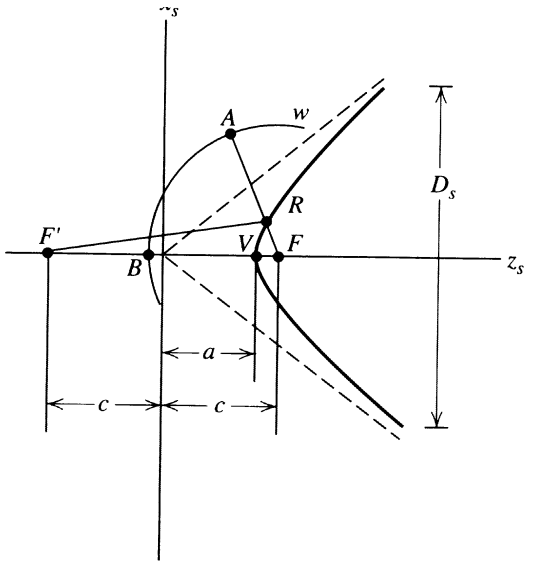

(*a*) Hyperbolic subreflector.

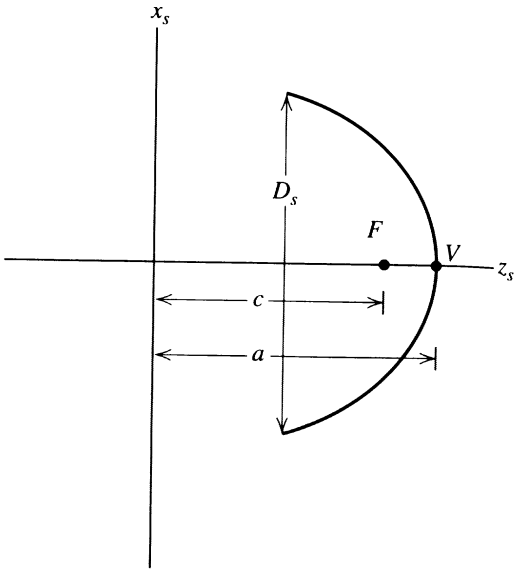

(*b*) Elliptical subreflector.

The subreflector is defined by its diameter D_s and its eccentricity e. The shape (or curvature) is controlled by the eccentricity:

$$e = \frac{c}{a}\begin{cases} > 1, & \text{hyperbola} \\ < 1, & \text{ellipse} \end{cases} \tag{14.40}$$

Special cases are

- $e = \infty$, straight line (plane)
- $e = 0$, circle (sphere)
- $e = 1$, parabola

Both, the ellipse and the hyperbola, are described by the equation:

$$\frac{z_s^2}{a^2} - \frac{x_s^2}{c^2 - a^2} = 1, \tag{14.41}$$

The function of a hyperbolic subreflector is to convert the incoming wave from a feed antenna located at the focal point F' to a spherical wave front *w* that appears to originate from the virtual

focal point F. This means that the optical path from F' to w must be constant with respect to the angle of incidence.

$$\overline{F'R} + \overline{RA} = \overline{F'V} + \overline{VB} = c + a + \overline{VB} \qquad (14.42)$$

Since

$$\overline{RA} = \overline{FA} - \overline{FR} = \overline{FB} - \overline{FR} \qquad (14.43)$$

($\overline{FA} = \overline{FB}$ because the reflected wave must be spherical)

$$\Rightarrow \overline{F'R} - \overline{FR} = c + a - (\overline{FB} - \overline{VB}) = c + a - (c - a) = 2a \qquad (14.44)$$

Note: Another definition of a hyperbola is: *a hyperbola is the locus of a point that moves so that the difference of the distances from its two focal points, $\overline{F'R} - \overline{FR}$, is equal to a constant, $2a$.*

Dual axisymmetric Cassegrain reflectors can be modeled as a single equivalent parabolic reflector as shown below.

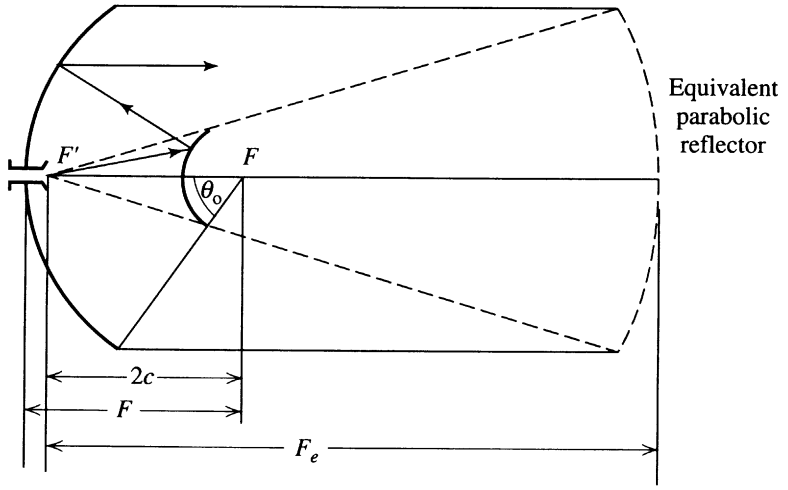

The equivalent parabola has the same diameter $D_e = D$ but its focal length is longer than that of the main reflector

$$F_e = \frac{e+1}{e-1} F = MF \qquad (14.45)$$

Here, $M = (e+1)/(e-1)$ is called magnification.

The increased equivalent focal length has several advantages:

- less cross-polarization
- less spherical-spread loss at the reflector's rim, and therefore, improved aperture efficiency.

The synthesis of dual-reflector systems is rather advanced topic. Many factors are taken into account when *shaped* reflectors are designed for improved aperture efficiency. These are minimized spillover, less phase error, improved amplitude distribution in the reflector's aperture.

7. Gain of reflector antennas

The maximum achievable gain for an aperture antenna is

$$G_{\max} = D_u = \frac{4\pi}{\lambda^2} A_p \qquad (14.46)$$

This gain is possible only if the following is true: uniform amplitude and phase distribution, no spillover, no ohmic losses. In practice, these conditions are not achievable, and the effective antenna aperture is less than its physical aperture:

$$G = \varepsilon_{ap} D_u = \frac{4\pi}{\lambda^2} \varepsilon_{ap} A_p, \qquad (14.47)$$

where $\varepsilon_{ap} \leq 1$ is the aperture efficiency. The aperture efficiency is expressed as a product of sub-efficiencies:

$$\varepsilon_{ap} = e_r \varepsilon_t \varepsilon_s \varepsilon_a \qquad (14.48)$$

where:

e_r is the radiation efficiency,
ε_t is the aperture taper efficiency,
ε_s is the spillover efficiency, and
ε_a is the achievement efficiency.

The taper efficiency can be found using the directivity expression for aperture antennas (see Lecture 12, Section 4):

$$D_0 = \frac{4\pi}{\lambda^2} \frac{\left| \iint_{S_A} \vec{E}_a ds' \right|^2}{\iint_{S_A} |\vec{E}_a|^2 \, ds'} \tag{14.49}$$

$$\Rightarrow A_{eff} = \frac{\left| \iint_{S_A} \vec{E}_a ds' \right|^2}{\iint_{S_A} |\vec{E}_a|^2 \, ds'} \tag{14.50}$$

$$\Rightarrow \varepsilon_t = \frac{A_{eff}}{A_p} = \frac{1}{A_p} \frac{\left| \iint_{S_A} \vec{E}_a ds' \right|^2}{\iint_{S_A} |\vec{E}_a|^2 \, ds'} \tag{14.51}$$

Expression (14.51) can be written directly in terms of the known feed antenna pattern. If the aperture is circular, then

$$\varepsilon_t = \frac{1}{\pi a^2} \frac{\left| \int_0^{2\pi} \int_0^a E_a(\rho', \varphi') \rho' d\rho' d\varphi' \right|^2}{\int_0^{2\pi} \int_0^a |E_a(\rho', \varphi')|^2 \, \rho' d\rho' d\varphi'} \tag{14.52}$$

Substituting $\rho' = r_f \sin\theta_f = 2F \tan(\theta_f / 2)$ and $d\rho' / d\theta_f = r_f$ in (14.52) yields:

$$\varepsilon_t = \frac{4F^2}{\pi a^2} \frac{\left| \int_0^{2\pi} \int_0^{\theta_o} F_f(\theta_f, \varphi') \tan\frac{\theta_f}{2} d\theta_f d\varphi' \right|^2}{\int_0^{2\pi} \int_0^{\theta_o} |F_f(\theta_f, \varphi')|^2 \sin\theta_f d\theta_f d\varphi'} \tag{14.53}$$

All that is needed to calculate the taper efficiency is the feed pattern $F_f(\theta_f, \varphi')$.

If the feed pattern extends beyond the reflector's rim, certain amount of power will not be redirected by the reflector, i.e. it will be lost. This power-loss is referred to as *spillover*. The spillover efficiency measures that portion of the feed pattern, which is intercepted by the reflector relative to the total feed power:

$$\varepsilon_s = \frac{\int_0^{2\pi} \int_0^{\theta_o} |F_f(\theta_f, \varphi')|^2 \sin\theta_f d\theta_f d\varphi'}{\int_0^{2\pi} \int_0^{\pi} |F_f(\theta_f, \varphi')|^2 \sin\theta_f d\theta_f d\varphi'} \tag{14.54}$$

The reflector design problem includes a trade-off between aperture taper and spillover through feed antenna choice. Taper and spillover efficiencies are combined to form the so-called *illumination efficiency* $\varepsilon_i = \varepsilon_t \varepsilon_s$. Multiplying (14.53) and (14.54), and using $a = 2F\tan(\theta_o/2)$ yields:

$$\varepsilon_i = \frac{D_f}{4\pi^2} \cot^2\frac{\theta_o}{2} \left| \int_0^{2\pi} \int_0^{\theta_o} F_f(\theta_f, \varphi') \tan\frac{\theta_f}{2} d\theta_f d\varphi' \right|^2 \tag{14.55}$$

Here,

$$D_f = \frac{4\pi}{\int_0^{2\pi} \int_0^{\pi} |F_f(\theta_f, \varphi')|^2 \sin\theta_f d\theta_f d\varphi'} \tag{14.56}$$

is the directivity of the feed antenna. An ideal feed antenna pattern would compensate for the spherical spreading loss by increasing

the field strength as θ_f increases, and then would abruptly fall to zero in the direction of the reflector's rim in order to avoid spillover:

$$F_f(\theta_f, \varphi') = \begin{cases} \dfrac{\cos^2(\theta_o/2)}{\cos^2(\theta_f/2)}, & \theta_f \le \theta_o \\ 0, & \theta_f > \theta_o \end{cases} \qquad (14.57)$$

This ideal feed is not realizable. For practical purposes, (14.55) has to be optimized with respect to the edge-illumination level. The function specified by (14.55) is well-behaved with a single maximum with respect to the edge-illumination.

The achievement aperture efficiency ε_a is an integral factor including losses due to: random surface error, cross-polarization loss, aperture blockage, reflector phase error (profile accuracy), feed phase error.

A well-designed and well-made aperture antenna should have an overall aperture efficiency of $\varepsilon_{ap} \approx 0.65$ or more, where "more" is less likely.

The gain of a reflector antenna will certainly depend on *phase errors*, which theoretically should not exist but are often present in practice. Any departure of the phase over the virtual aperture from the uniform distribution leads to a significant decrease of the directivity. For paraboloidal antennas, phase errors result from:

- displacement of the feed phase centre from the focal point;
- deviation of the reflector surface from the paraboloidal shape, including surface roughness and other random deviations;
- feed wave fronts are not exactly spherical.

Simple expression has been derived[1] to predict with reasonable accuracy the loss in directivity for rectangular and circular apertures when the peak value of the aperture phase deviations is known. Assuming that the maximum radiation is along the reflector's axis, and assuming a maximum phase deviation *m*, the ratio of the directivity without phase errors D_0 and the directivity with phase errors *D* is given by:

$$\frac{D}{D_0} \geq \left(1 - \frac{m^2}{2}\right)^2 \tag{14.58}$$

The maximum phase deviation *m* is defined as:

$$|\triangle\phi| = |\phi - \bar{\phi}| \leq m \tag{14.59}$$

where ϕ is the aperture's phase function, and $\bar{\phi}$ is its average value.

[1] D.K. Cheng, "Effects of arbitrary phase errors on the gain and beamwidth characteristics of radiation pattern," *IRE Trans. AP*, vol. AP-3, No. 3, pp. 145-147, July 1955.